Energetic ion losses caused by MHD activity resonant and non-resonant with energetic ions in LHD

Kunihiro Ogawa[1], Mitsutaka Isobe[1,2], Kazuo Toi[1], Akihiro Shimizu[1], Donald A. Spong[3], Masaki Osakabe[1], Satoshi Yamamoto[4] and LHD experiment group[1]

[1] *National Institute for Fusion Science, Toki, 509-5292, Japan.*

[2] *The Graduate University for Advanced Studies, Toki, 509-5292, Japan*

[3] *Oak Ridge National Laboratory, Oak Ridge, Tennessee, 37831, USA.*

[4] *Institute of Advanced Energy, Kyoto University, Uji, 611-0011, Japan.*

First author's email address: ogawa.kunihiro@lhd.nifs.ac.jp

Abstract

Experiments to reveal energetic-ion dynamics associated with magnetohydrodynamic (MHD) activity are ongoing in the large helical device (LHD). Interactions between beam-driven toroidal Alfvén eigenmodes (TAEs) and energetic ions have been investigated in LHD. Energetic-ion losses induced by beam-driven bursts TAEs have been observed by using a scintillator-based lost fast-ion probe (SLIP) in neutral beam-heated high β plasmas. The loss flux of co-going beam ions increases as the TAE amplitude increases. In addition to this, expulsion of beam ions associated with edge localized modes (ELMs) has been also recognized in LHD. The SLIP has indicated that beam ions having co-going and barely co-going orbits are affected by ELMs. The relation between ELM amplitude and ELM-induced loss has a dispersed structure. To understand the energetic-ion loss process, a numerical simulation based on an orbit-following model, DELTA5D that incorporates magnetic fluctuations is performed. The calculation result shows that energetic ions confined in the interior region are lost due to the TAE instability with a diffusive process characterizing their loss. For the ELM, energetic ions existing near the confinement/loss boundary are lost through a convective process. We found that the ELM-induced loss flux measured by SLIP changes with ELM phase. This relation between the ELM amplitude and measured ELM-induced loss results in a more dispersed loss structure.

Keywords: Energetic ion, toroidal Alfvén eigenmode, Edge localized mode, Lost-fast ion diagnostics, Orbit simulation

PACS: 52.35.Bj, 52.25.Gj, 52.55.Pi, 52.55.Hc, 52.25.Fi

1. Introduction

To realize a self-sustained D-T burning plasma, fusion-born energetic alpha particles (α's) should be confined long enough to heat the bulk plasma [1]. In addition to this, loss of α's should be controlled since the localized loss might damage plasma facing components. Better understanding of the transport and loss of these energetic ions is therefore essentially required to realize a nuclear fusion reactor. The principal concern is that D-T produced α's and super-Alfvénic ions such as beam ions destabilize energetic-ion-driven magnetohydrodynamic (MHD) instabilities such as Alfvén eigenmodes (AEs) [2] because those instabilities can potentially cause losses of energetic ions through wave-particle resonance. Recently, the effect of MHD mode non-resonant interactions with energetic ions such as edge localized mode (ELM) [3] is also of great concern since the transport of energetic ion may be affected through not only wave-particle resonance but also stochastization of energetic-ion orbits [4].

Energetic-ion losses due to MHD instabilities have been studied intensively in mid to large-sized tokamaks [1]. Previously, detailed loss processes of energetic ions due to AEs were studied in TFTR [5]. In those experiments, due to global AE, decreases of neutron emission rate, and at the same time, increase of beam-ion losses were observed [6]. On the other hand, energetic-ion losses induced by MHD activity that is non-resonant with the energetic ions, such as sawteeth or tearing mode, were studied [7, 8]. Recently, ELM-induced beam-ion losses have been measured in ASDEX-U, DIII-D, and KSTAR [9, 10]. These experiments reported that the amplitude of energetic-ion loss increases towards the ELM crash while the density fluctuation amplitude due to the ELM does not. So, the loss process of energetic ions due to the ELM is still not clear yet.

It is also important for helical/stellarator plasmas understand the loss process of energetic ions caused by MHD activities. It is not only for finding a way to realize a helical/stellarator reactor but also to obtain a deeper understanding of the energetic-ion loss due to MHD activity in toroidal devices. AE-induced energetic-ion loss has been studied in the compact helical system (CHS) [11], Wendelstein 7-AS [12] and the large helical device (LHD) [13]. Previously, in CHS, they reported that the energetic-ion flux would be dependent on the mode structure and mode amplitude levels [11]. Observation of energetic-ion losses induced by the resistive interchange mode, which was non-resonant with the energetic ions was reported in LHD [13]. It was shown that the energetic ions would be lost through a convective process. Recently, measurement of ELM structure and study on the characteristics of ELMs has been

performed in LHD [14, 15]. However the effect of ELMs on energetic-ion loss in three-dimensional magnetic field is not clear yet. In tokamaks, externally-applied three-dimensional magnetic fields are intensively used to mitigate ELMs [16-19]. Understanding the fast-ion loss process due to ELM in the LHD will contribute the understanding of ELM-induced fast-ion loss in tokamak plasmas with externally-applied three-dimensional magnetic fields. In this paper, we present results on the characteristics of energetic-ion losses due to both TAE and ELM instabilities. Comparison between the TAE and ELM induced losses gives us a deeper understanding of the energetic-ion loss process.

2. Experimental setups

LHD is classified into heliotron device. It is the world-largest heliotron device; its major radius and an average minor radius (a) are 3.90 m and 0.6 m, respectively. The direction of toroidal magnetic field is changeable due to change of external helical coil current. In experiments described in this paper, the toroidal magnetic field (Bt) is in the counterclockwise direction, looking down from the top view. Three negative-source based neutral beam injectors (NB1 to NB3) and two diagnostic neutral beam injectors (PNB) are equipped with LHD. In this experiment, NB1 produces super Alfvénic beams injected in the co-direction. NB1 injects hydrogen beams with injection energy of 180 keV. We use a scintillator-based lost-fast ion probe (SLIP) to measure the lost-fast ions in this experiment. Figure 2 a) shows the model of head section of SLIP. This instrument is essentially a magnetic spectrometer based on the LHD magnetic field, and consists of a pair of apertures and a scintillator plate. We use 4x4 photomultipliers (PMTs) to measure the time evolution of scintillation light due to the bombardment of energetic ions with fine time resolution (up to 5 μs). The detailed structure and function of the SLIP are described in Refs. 20 and 21. Figure 2 shows the sight lines of fast-time response Hα array (FHA). We used channel one of FHA to measure ELM. The poloidal magnetic fluctuation amplitude of the TAE ($b_{\theta TAE}$) or ELM ($b_{\theta ELM}$) is measured by a Mirnov coil (MP) placed on the vacuum vessel. The toroidal mode number (n) and poloidal mode number (m) of the MHD modes are identified using signals from the Mirnov coil arrays. The electron temperature (T_e) and the electron density (n_e) profiles are provided by Thomson scattering diagnostics [22]. The line-averaged density ($<n_e>$) is measured with a multi-channel far-infrared laser interferometer [23].

3. Experimental results

Study on TAE and ELM induced loss is performed in NB-heated LHD plasmas. Figure 3 shows the time evolution of absorbed power of NB (P_{NBabs}), electron temperature at the center

(T_{e0}), $<n_e>$, volume-averaged beta value $<\beta>$ and frequency spectrogram of MP signal of a typical discharge in which TAEs and ELMs co-exist. The magnetic configuration are Bt=0.9T, Rax=3. 90 m and γ=1. 2. In this discharge, plasma is start up and sustained by NB1. The beams injected by NB1 are super Alfvénic (the ratio of the initial energetic-ion velocity to the Alfvén speed is ~1.5). Note that PNB having an injection energy of 40 keV is perpendicularly injected for diagnostics. In this experiment, typical value of T_{e0}, $<n_e>$ and $<\beta>$ are 0.6 keV, ~2.0×10^{19}m^{-3} and ~0.5 %, respectively. MP signal analysis shows that strongly-excited TAE having 20~40 kHz is existing at t~4.0 s to 4.7 s (Fig.3). The toroidal and poloidal mode numbers are n=1 and m=1+2, respectively. The amplitude of the mode at the MP position is ~2.0×10^{-5} T at t=4.2 s. Figure 4a shows the time evolution of the magnetic fluctuations in the TAE range of frequency measured by MP and the signal of lost-fast ion ($\Gamma_{\text{fast ion}}$) having the energies (E) in the range of 40-160 keV and χ in the range of 20-30 degrees. Note that increases in loss flux due to TAE bursts are clearly observed only in this E and χ ranges. The increment of loss flux ($\Delta\Gamma_{\text{fast ion}}$) as a function of $b_{\theta\text{TAE}}/Bt$ is shown in Fig. 4 b. It shows that $\Delta\Gamma_{\text{fast ion}}$ increases with TAE amplitude as expected.

Also low-frequency fluctuations less than 20 kHz are seen in Fig. 3. The Mirnov array reveals that this mode has a structure of m/n=1/1. The lower frequency mode is identified as an ELM. Such instabilities are observed an LHD plasma having a steep pressure gradient [14]. Unlike tokamaks, the elms are the result of non-linear growth of the resistive interchange mode [15]. The fluctuation amplitude of the ELM at MP position is 2x10^{-4} T. Time evolution of magnetic fluctuations in the ELM frequency range measured by MP, Hα signal, and $\Gamma_{\text{fast ion}}$ having the E of 160-180 keV and χ of 40-50 degrees are shown in Fig 5 a. Due to the ELM burst, increases of Hα and lost-fast ion signal are seen. We choose this $\Gamma_{\text{fast ion}}$ because large increases of fast-ion loss are seen in this range of E and χ. Note that the increases of loss due to ELM are seen on all E and χ ranges can be measured by SLIP. The $\Delta\Gamma_{\text{fast ion}}$ as a function of b_{ELM}/Bt is shown in Fig. 5 b. Plots of energetic-ion loss as a function of ELM amplitude indicate a dispersed structure.

4. Setups for orbit following models

To understand the TAE or ELM induced loss, orbit following simulation including TAE or ELM fluctuation is performed. DELTA5D code [24] is used to follow the fast ion orbit inside the LCFS based on equilibrium reconstructed by VMEC2000 code [25] including time and frequency varying magnetic fluctuation (detail of fluctuations is described in next paragraph). Birth profile of beam ions are calculated by the HFREYA code [26] (Fig. 6 a). We use the Lorentz orbit code to follow the fast-ion orbit outside the LCFS because DELTA5D calculate

the orbit by means of equilibrium reconstructed by VMEC2000 code which reconstructs the equilibrium inside the LCFS.

In DELTA5D, the magnetic fluctuation is modeled as $\boldsymbol{b}= \nabla\times(\alpha\boldsymbol{B})$. Here, α represents a general function of the position, frequency, and amplitude of the magnetic fluctuation. According to the magnetic fluctuation amplitude measured by an MP, the amplitude of α is obtained [27, 28]. In the TAE case, the shear Alfvén continuum is calculated by the STELGAP code [29] (Fig. 6 b). The radial structure of α is obtained from the eigenfunction of a stable TAE mode calculated by AE3D model [30], as shown in Fig. 6 c. The TAEs have a mode structure of m/n=1+2/1 and have a peak at r/a~0.6. Note that the profile of n_e fluctuations due to the TAE (evaluated from AE3D) eigenfunction agrees well with that measured in previous experiments [13]. The frequency of α and frequency down-chirping rate are set to be 20 kHz and 20 kHz/ms, respectively as seen in the experimentally observed TAE burst. Figure 6 d shows the radial structure of α for an ELM. It is given based on effective region of ELM measured by TSD (Fig. 6 e and f). The ELM has a mode structure of m=1 and n=1 and is characterized by a relatively narrow radial profile.

5. Result of orbit calculation

Figure 7 shows the increment of energy-ion loss as a function of TAE amplitude from the calculation. It shows that $\Delta\Gamma_{\text{fast ion}}$ increases quadratically with b_{TAE}/Bt; the tendency agrees with experimental results. The quadratic dependence shows that energetic ions in interior region are lost from the plasma with a diffusive process [28, 31]. The increment of energetic-ion loss as a function of ELM amplitude is shown in Fig. 8. Energetic-ion loss increases almost linearly with *beam*/*but* when we fix an initial phase of ELM. This tendency shows that energetic ions near the confinement/loss boundary are mainly lost through a convective process [28, 31]. We found that ELM-induced energetic-ion loss depends on the mode phase of the ELM. In experiments, the ELM could take on any initial phases; therefore, this is roughly consistent with the dispersed structure observed experimentally. However, the phase effect shown in Fig. 9 seems to be small compared with the observed scattering of the data shown in Fig. 8. Large magnetic fluctuations related to ELMs may modify the MHD equilibrium structure near the edge appreciably. Such an effect might be an additional candidate to get a better agreement between experimental and calculated results.

Let us discuss the reason why an ELM phase affects the energetic-ion loss. Figure 9 shows the exit point of energetic ion on the LCFS due to the TAE and ELM as a function of poloidal angle. It shows that in ELM case, the poloidal distribution of energetic ion is largely changed due to the initial phase of the mode compared with TAE case. In this experiment, the

frequency of the ELM is much lower than the orbital frequency of the energetic ions. Then loss points of energetic ions can be largely changed toroidally or poloidally due to ELM phases because the shape of fluctuation does not change during the toroidal or poloidal transit time of the fast ions. In Fig. 9, the detectable region of the SLIP on the LCFS is overlaid. Because of the choice $\gamma = 1.20$, the SLIP only can cover from -180 degrees to -60 degrees and 60 degrees to 180 degrees in poloidal angle on the LCFS. Due to this fact, the energetic-ion loss depends on the phase of the ELM fluctuations.

6. Summary

To understand the loss processes of energetic ion caused by MHD activities that are both resonant and non-resonant with energetic ion orbits, energetic-ion losses are measured with a SLIP on a discharge in which TAEs and ELMs co-exist. The E and χ resolved measurements of energetic ion losses indicate that TAE induces co-going energetic ion losses whereas the ELM induces a loss of energetic ions having co-going and barely co-going orbits. In the TAE case, the energetic-ion loss flux increases with an increase of the magnetic fluctuation amplitude. On the other hand, in the ELM case, a plot of the loss flux of energetic ions as a function of magnetic fluctuation amplitude has a more dispersed structure. To understand the difference between TAE-induced energetic-ion loss and ELM-induced energetic ion loss, orbit following simulations including magnetic fluctuations is performed. In this calculation, a radial profile of a TAE mode is given based on the stable eigenfunction whereas a radial profile of an ELM is constructed based on experimental observation. The result shows that the TAE-induced loss increases quadratically with the magnetic fluctuation amplitude of the TAE. This qualitatively agrees with experimental results. The dependence of ELM-induced energetic-ion losses as a function of the ELM amplitude used in the calculation shows that it has a linear dependence. We found that the effect of the ELM phase on the energetic-ion loss gives the dependence of the loss vs. the amplitude a more dispersed structure, because the initial phase of an ELM changes poloidal distribution of fast-ion loss.

Acknowledgement

This work was supported in part by the Grant-in-Aid for Scientific Research from JSPS Nos. 21360457 and 21340175, and from the LHD project budget (NIFS13ULHH003). The authors are grateful to the LHD operation group for their excellent technical support.

Reference

[1] Fasoli A., Gormenzano C., Berk H. L. *et al*. 2007 Nucl. Fusion **47** S264

[2] Chen C. Z. and Chance M. S. 1986 Phys. Fluids **29** 3695
[3] Zohm H., 1996 Plasma Phys. Control. Fusion **38** 105
[4] Mynick H. E., 1993 Phys. Fluids B **5** 5
[5] Zweben S. J., 1989 Nucl. Fusion **29** 5 825
[6] Darrow D. S., Zweben S. J., Chang Z. *et al* 1997 Nucl. Fusion **37** 7 939
[7] Stratton B. C., Fonck R. J., Mckee G. R. *et al* 1996 Nucl. Fusion **36** 11 1586
[8] García-Muñoz M., Martin P., Fahrbach H. U. *et al* 2007 Nucl. Fusion **47** L10
[9] García-Muñoz M., Akaslompolo S., Asunta O. *et al* 2013 Nucl. Fusion **53** 123008
[10] Chen X., Austin M. E., Fisher R.K. *et al*., 2013 Phys. Rev. Lett. **110** 065004
[11] Isobe M., Toi K., Matsushita H. *et al* 2006 Nucl. Fusion **46** S918
[12] Weller A., Anton M., Geiger J. *et al* 2001 Phys. Plasmas **8** 931
[13] Ogawa K., Isobe M., Toi K. *et al* 2010 Nucl. Fusion **50** 084005
[14] Watanabe F., Toi K., Ohdachi S. *et al* 2006 Plasma Phys. Control. Fusion **48** A201
[15] Toi K., Ohdachi, S., Suzuki, Y. *et al* 2014 Nucl. Fusion **54** 033001
[16] Hender T. *et al* 1992 Nucl. Fusion **32** 2091
[17] Evans T. *et al* 2004 Phys. Rev. Lett. **92** 235003
[18] Liang Y. *et al* 2007 Phys. Rev. Lett. **98** 265004
[19] Suttrop W. *et al* 2011 Phys. Rev. Lett. **106** 225004
[20] Ogawa K., Isobe M. and Toi K. 2009 J. Plasma Fusion Res. Series **8** 655
[21] Ogawa K., Isobe M. and Toi K. 2008 Plasma Fusion Res. **3** S1082
[22] Yamada I., Narihara K., Funaba H. *et al* 2010 Fusion Sci. Tech. **58** 345
[23] Akiyama T., Kawahata K., Tanaka K. *et al* 2010 Fusion Sci. Tech. **58** 352
[24] Spong D. A. 2011 Phys. Plasmas **18** 056109
[25] Hirshman S. P. and Betancourt O. 1991 J. Comput. Phys. **96** 99
[26] Murakami S., Nakajima N., Okamoto M. *et al* 1995 Trans. Fusion Technol. **27** 256
[27] Ogawa K., Isobe M., Toi K. *et al* 2012 Nucl. Fusion **52** 094013
[28] Ogawa K., Isobe M., Toi K. *et al* 2013 Nucl. Fusion **53** 053012
[29] Spong D.A., Sanchez R. and Weller A. 2003 Phys. Plasmas **10** 3217
[30] Spong D. A., D'azevedo E. and Todo Y. 2010 Phys. Plasmas **17** 022106
[31] Sigmar D. J., Hsu C. T., White R. B. *et al* 1992 Phys. Fluids B **4** 6

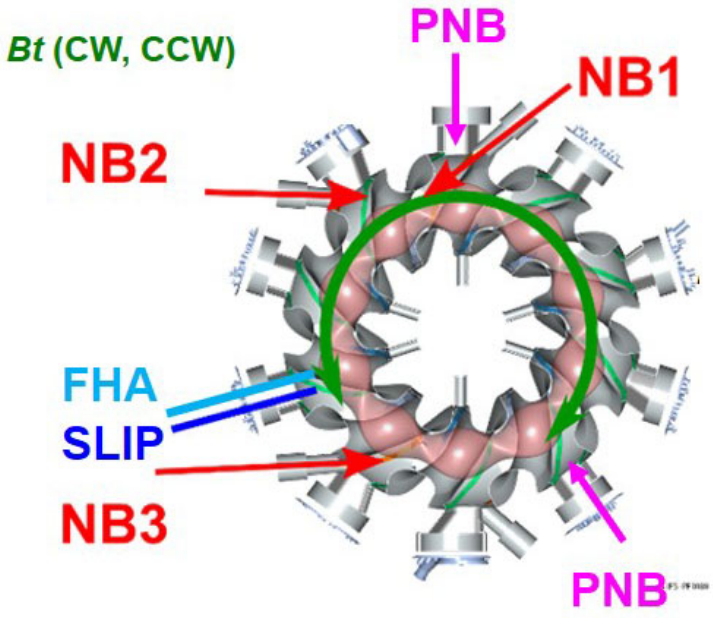

Fig. 1 Toroidal magnetic field direction can be changed by changing of helical coil current direction. Three tangential NBs (NB1, NB2 and NB3) and two perpendicular NBs (PNB) are equipped with LHD. Injection energy of NB1 to NB3 and PNBs are 180 keV and 40 keV, respectively. Fast-time-response Ha detector array (FHA) and scintillator-based lost-fast ion probe (SLIP) are installed outboard side of the torus.

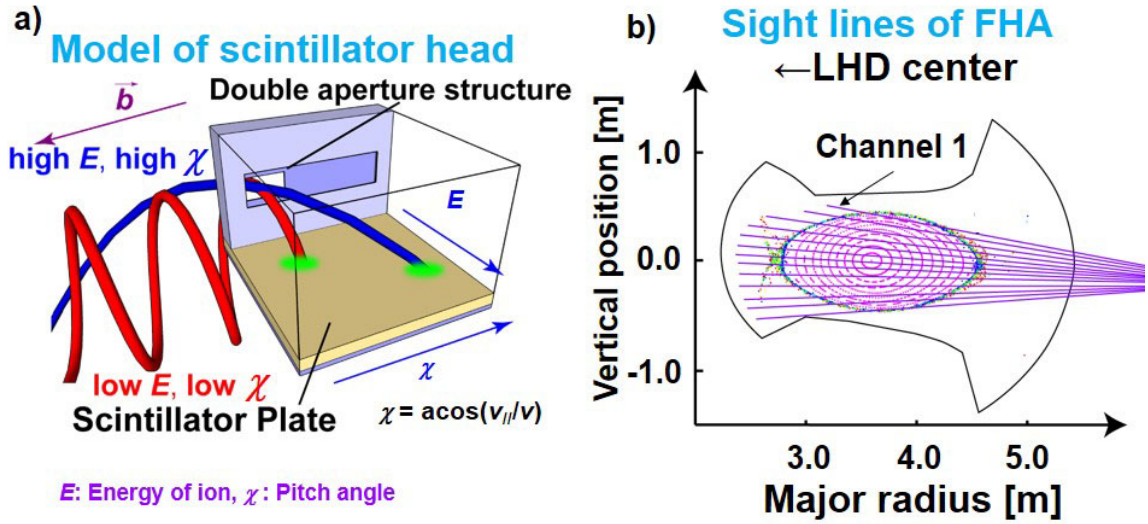

Fig. 2 a) Model of head section of scintillator-based lost-fast ion probe (SLIP). It can discriminate the energy of fast ions entering through the double aperture. b) Sight lines of fast-time-response Ha detector array (FHA). We use channel one in this paper.

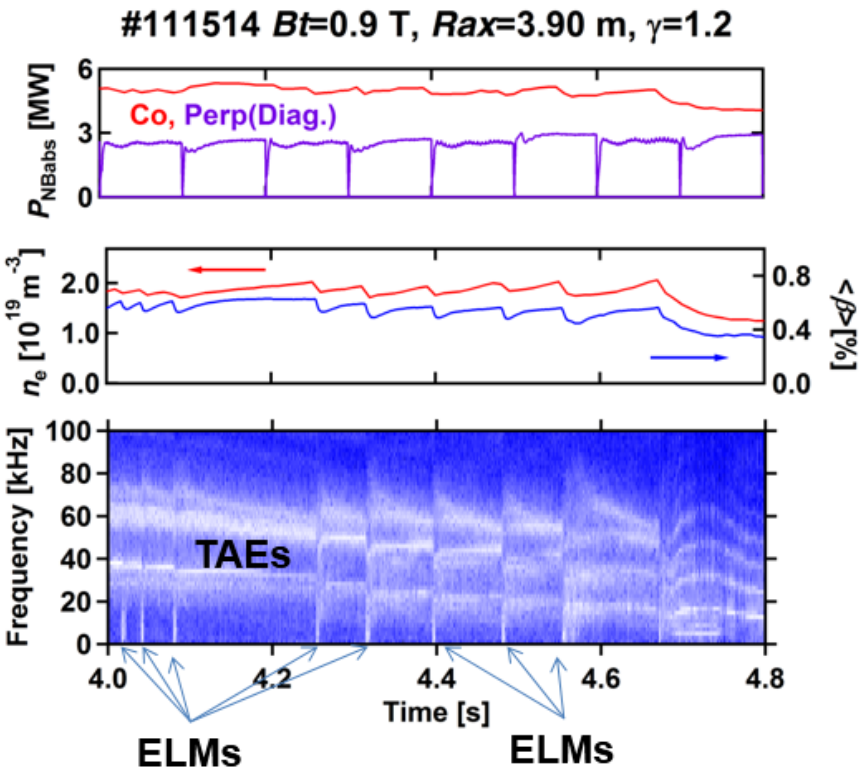

Fig. 3 Time trace of absorbed power of neutral beam injection (P_{NBabs}) of NB1 and diagnostic beams, line averaged density, volume averaged beta and power spectrogram of Mirnov signal on typical discharge with TAEs and ELMs.

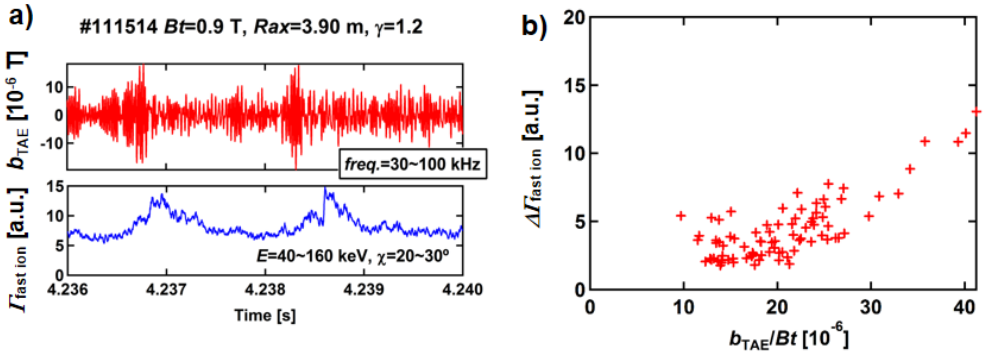

Fig. 4 a) Typical time traces of magnetic fluctuation of a TAE range of frequency and signal of lost-fast ion (b_{TAE}). b) Increment of fast-ion loss as a function of TAE amplitude measured at magnetic probe position normalized by toroidal magnetic field strength. Increment of fast-ion loss increase with TAE amplitude.

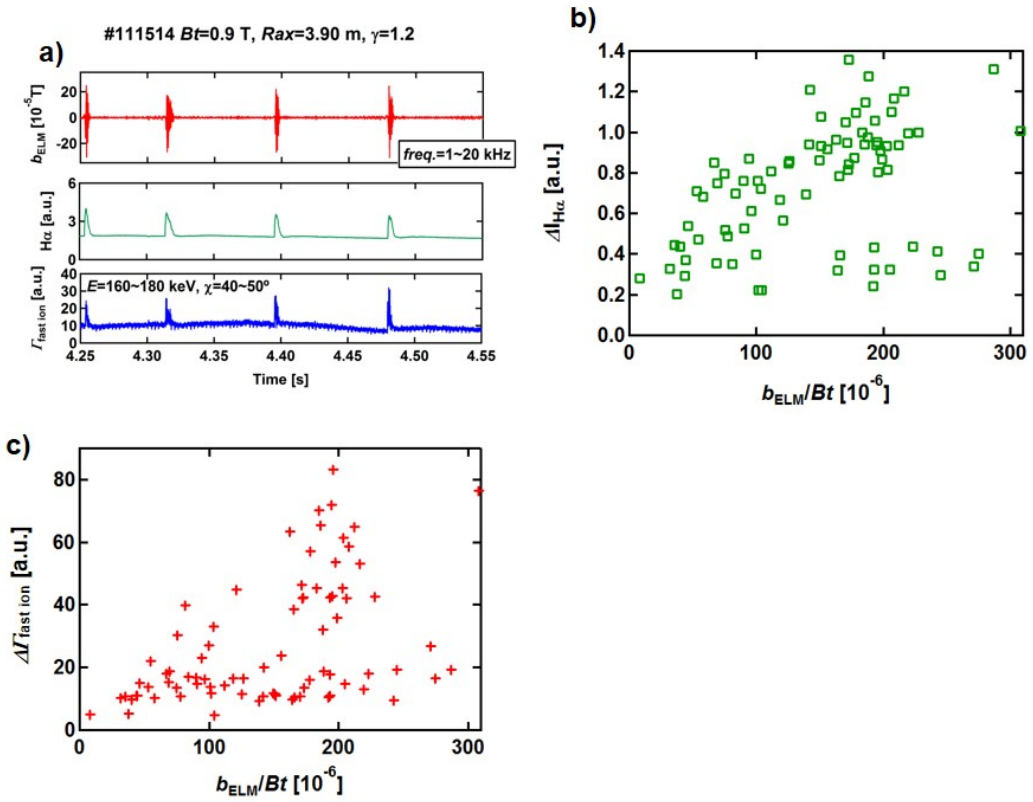

Fig. 5 a) Typical time traces of magnetic fluctuation of ELM range of frequency, Hα signal, and signal of lost-fast ion. b) Increment of Hα signal as a function of ELM amplitude measured at magnetic probe position (b_{ELM}) normalized by toroidal magnetic field strength. There are no clear dependence. c) Increment of fast-ion loss as a function of b_{ELM}/Bt. It has a dispersed structure.

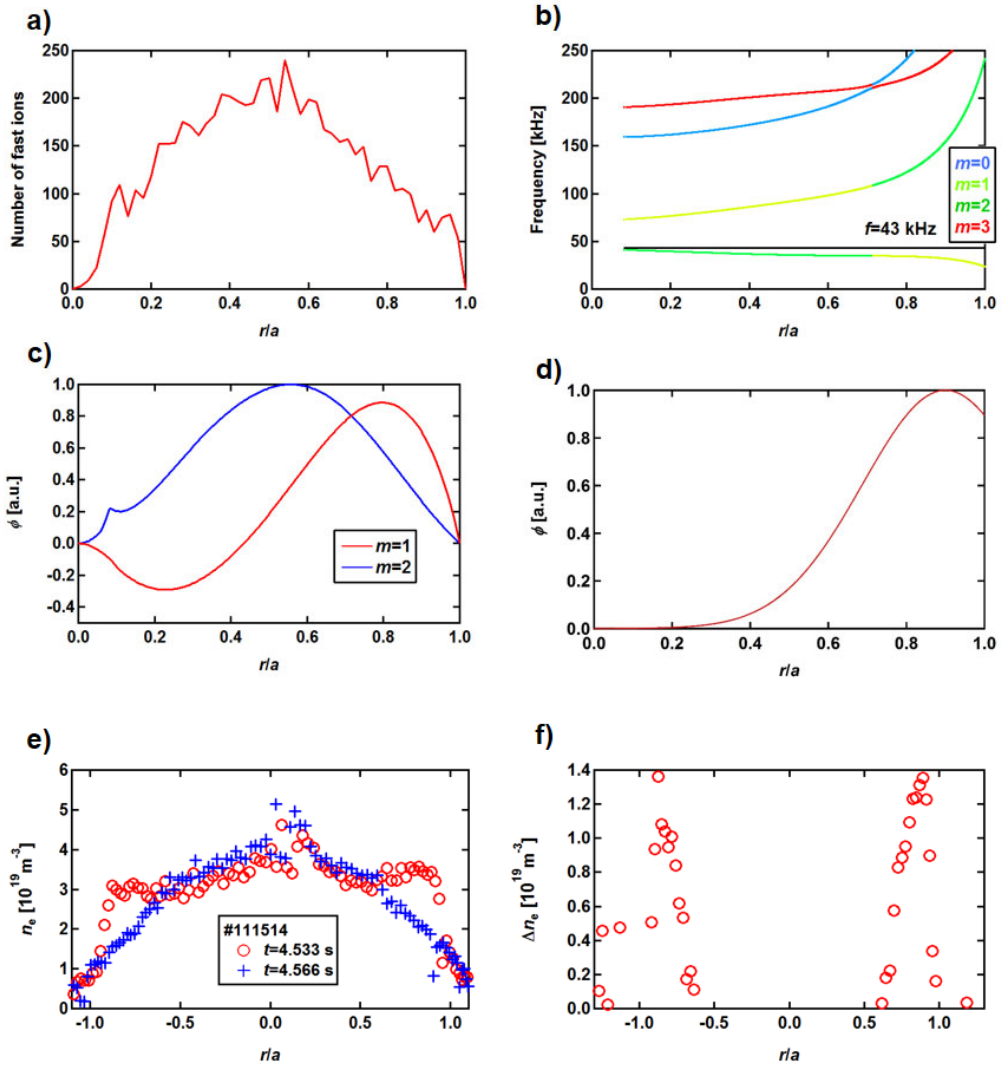

Fig. 6 a) Birth profile of beam ions calculated by HFREYA code. b) Shear Alfvén spectra calculated by the STELGAP code at t=4.0 s. c) Eigenfunction of TAE as a function of normalized minor radius. The profile is calculated using AE3D code. d) Eigenfunction of ELM as a function of normalized minor radius. The profile is given according to experimental observation. e) Electron density profile measured by TSD before (t=4.533 s) and after the ELM (t=4.566 s). Here, negative r/a means the inboard side of a plasma whereas positive r/a means outboard side of the plasma. f) Radial profile of decrement of electron density due to an ELM burst. We refer this profile as a radial ELM profile in calculation.

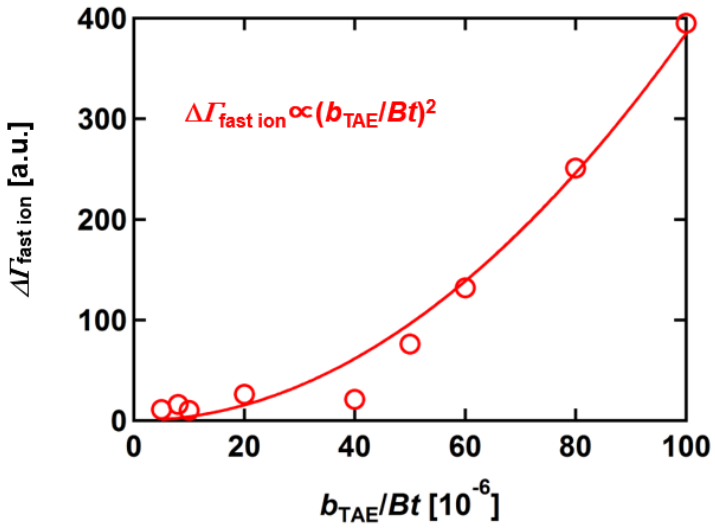

Fig. 7 Increment of fast-ion loss as a function of TAE amplitude at the magnetic probe position from the calculation. The incremental loss of fast-ions increases quadratically with the TAE amplitude.

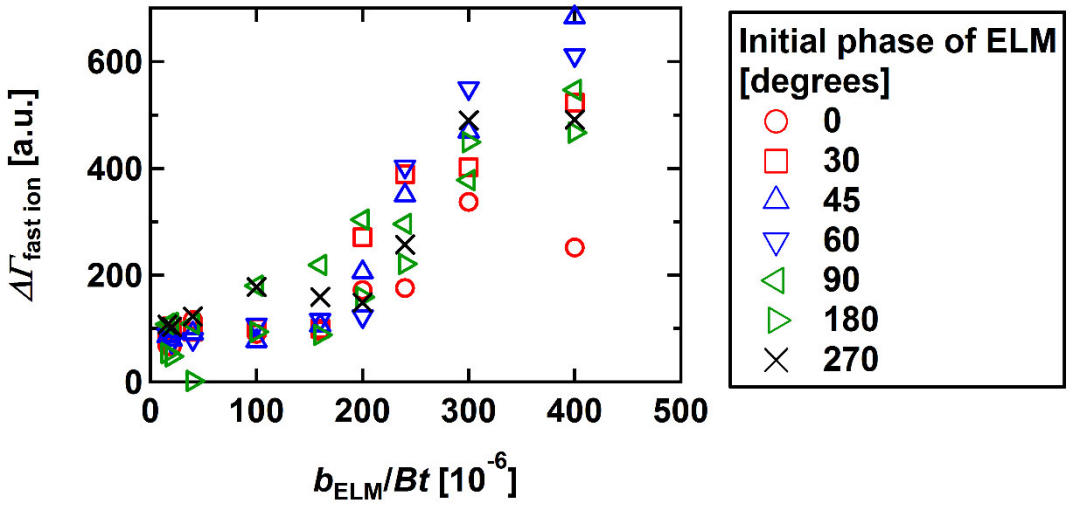

Fig. 8 Increment of energetic-ion loss as a function of ELM amplitude at the magnetic probe position from the calculation. The incremental loss of energetic-ions increases almost linearly with ELM amplitude in each case. Energetic ion loss is dependent on the initial phase of ELM.

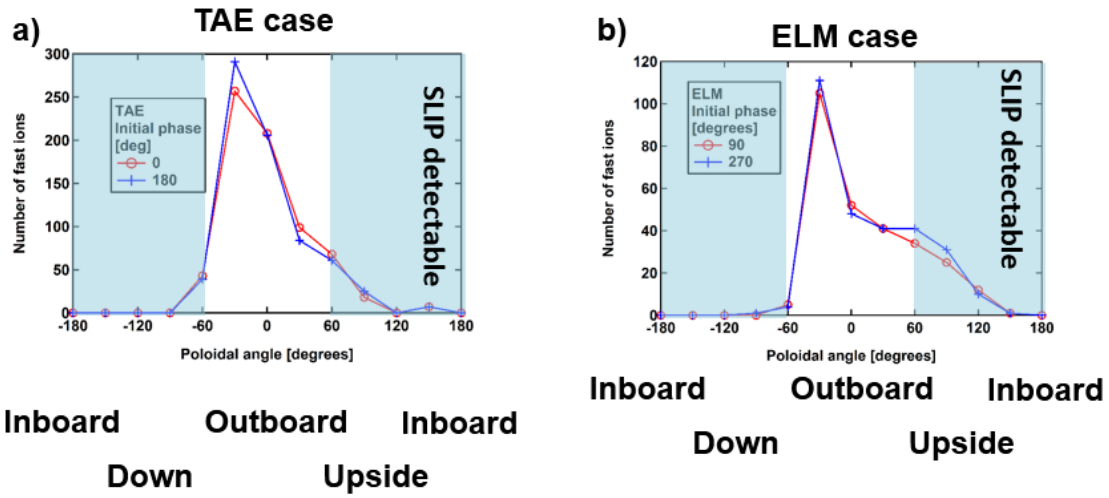

Fig. 9 histograms of the poloidal distribution of exit points of fast ions on the LCFS due to a) TAE or b) ELM together with the detectable region of SLIP.